

Cavity Ring-Down and Cavity-Enhanced Detection Techniques for the Measurement of Aerosol Extinction

Hans Moosmüller, Ravi Varma, and W. Patrick Arnott

Desert Research Institute, University of Nevada System, Reno, Nevada, USA

An instrument employing cavity ring-down (CRD) and cavity-enhanced detection (CED) for the local measurement of aerosol extinction is described and demonstrated. CRD measures the lifetime of photons in a high-quality optical cavity and thereby determines the sum of sample extinction between the cavity mirrors and that due to mirror losses. CRD systems can be calibrated with a single gas for the determination of extinction. A green laser emitting subnanosecond pulses is used as a light source, facilitating measurements free from optical interference in the cavity. The addition of a low-frequency chopper allows for the determination of extinction coefficients with simple linear fitting procedures and also facilitates CED measurements by providing laser power modulation for phase-sensitive detection. CED measures the average power transmitted by the optical cavity. After calibration with two gases, CED allows for the independent measurement of extinction with very high dynamic range and for an independent comparison with CRD measurements, thereby increasing confidence in the measurements.

INTRODUCTION

The atmospheric extinction of electromagnetic waves in the visible and near-visible spectral regions influences the earth's climate by changing short-wave radiative forcing (Jain et al. 2000; Reddy and Venkataraman 2000) and influences optical remote sensing by ground-based, airborne, and satellite systems (Schott 1997), including visual perception by humans (Chow

et al. 2002; Watson 2002). Optical extinction in the atmosphere is due to scattering and absorption by both particle-free air and aerosols. The scattering and absorption of light by particle-free air is attributed to its gaseous components and seems to be well understood and modeled (Bates 1984; Chetwynd et al. 1994; Bucholtz 1995; Rothman et al. 1998; Lubin et al. 2000).

The lower limit of atmospheric extinction is largely due to Rayleigh scattering of particle-free air, resulting in an extinction of 12.1 Mm^{-1} in the green (i.e., 550 nm) at standard temperature and pressure (STP; 273.2 K and 101.32 kPa; Anderson et al. 1996). Additional atmospheric extinction in this wavelength region can be caused by nitrogen dioxide ($0.26 \text{ Mm}^{-1}/\text{ppb NO}_2$ at 550 nm; e.g., Davidson et al. 1988), to a lesser degree by ozone ($0.009 \text{ Mm}^{-1}/\text{ppb O}_3$ at 550 nm; e.g., Brion et al. 1998), and by aerosol, which tends to be spatially and temporally inhomogeneous. The instrumental challenge is to measure aerosol light extinction with an accuracy better than about 10% of the Rayleigh background level. Therefore, the instrument has to be capable of a sensitivity of about 1 Mm^{-1} , corresponding to a 1 ppm change in optical power over 1 m. As it is difficult to measure a power change on the order of 1 ppm, much longer path lengths are being used. For example, the IMPROVE program of the U.S. National Park Service uses transmissometers with multiple kilometer path lengths to monitor atmospheric extinction continuously in remote Class I wilderness areas and National Parks (Molenar et al. 1989). While the long path length leads to high sensitivity, it also causes data loss and potential systematic errors due to atmospheric optical turbulence and thermal lensing, and makes it difficult to find good instrument sites and to move instruments to different locations. In addition, the absorption and scattering components of atmospheric extinction are commonly determined with local measurements making comparisons with the long path-integrated extinction measurements difficult.

An obvious solution to this dilemma is to implement a long, multiple kilometer path length in a compact (e.g., $\approx 1 \text{ m}$ length) cell with highly reflecting mirrors. Conventional multipass cells separate the individual reflections spatially with each reflection occurring on a different spot of the mirror (Herriott and Schulte 1965; White 1976). The laser beam is extracted after a given

Received 29 July 2004; accepted 27 October 2004.

This work has been supported in part by the National Science Foundation (ATM-9871192), the U.S. Department of Energy Pacific Northwest National Laboratory (3492), the U.S. Department of Agriculture Forest Service Rocky Mountain Research Station (03-JV-11222049-102), the U.S. Department of Defense (SERDP CP-1191), and by the Applied Research Initiative of the State of Nevada. It is a pleasure to thank all participants in the Reno Aerosol Optics Study (RAOS) and the Combustion Aerosol Optics Study (CAOS) in Missoula for their support with these experiments.

Address correspondence to H. Moosmüller, Desert Research Institute, University of Nevada System, 2215 Raggio Parkway, Reno, NV 89512, USA. E-mail: hansm@dri.edu

number of roundtrips, as limited by the available mirror area. An astigmatic variant of the Herriot cell has yielded 182 passes for a total path length of 100 m, based on a mirror separation of 0.55 m (McManus et al. 1995).

Even larger path lengths can be obtained if the distance traveled in the cell is not obtained from the spatial location of the laser beam but from the time it has been confined in the cell. Such systems can overlap all passes in space and are commonly referred to as Cavity Ring-Down (CRD) systems. The simplest implementation of CRD uses a stable two-mirror resonator with periodic injection of a laser pulse. If the laser pulse is shorter than the cavity's roundtrip time, no interference occurs. The optical energy stored in the cavity decays exponentially with time due to extinction between the two mirrors and due to reflection losses at the mirrors (O'Keefe and Deacon 1988; Ramponi et al. 1988). Measuring the optical power leaking out of the cavity through the second mirror, the exponential decay can be monitored and its decay constant calculated. If the mirror losses are constant in time, they can be measured, for example, by evacuating the cavity and subtracting the mirror losses from the decay constant. After such a calibration, CRD gives an absolute measurement of extinction between the two mirrors (Romanini et al. 1997).

Instead of measuring the decay constant of the optical energy stored in the cavity between laser pulses (CRD), the power transmitted through the cavity averaged over many laser pulses can be measured to obtain the optical extinction sensitively with long path length. This alternative or complimentary approach is known for example as cavity enhanced detection (CED) and can yield a larger dynamic range and less potential for systematic errors than CRD. For our setup, the laser pulse is shorter than the cavity's roundtrip time, and CED can be added to our CRD system with very little effort. For continuous-wave single-mode lasers, on the other hand, the cavity longitudinal mode structure must be taken into account, necessitating a more complex setup that either locks cavity and laser modes together (Ye et al. 1996) or utilizes off-axis beam paths (Paul et al. 2001). To avoid the need to lock cavity and laser modes together, the sample can also be directly introduced into the laser cavity yielding an intracavity technique (Knollenberg 1982). In this case calibration

must take the interaction of laser gain and sample extinction into account. (Demtröder 2002).

It has been noticed early on that ambient aerosol can contribute significantly to the CRD signal (Ramponi et al. 1988), but CRD systems have been used only recently to monitor aerosols (Sappey et al. 1998) and their extinction (Smith and Atkinson 2001; Strawa et al. 2002; Thompson et al. 2002). In the following, we discuss a unique hybrid CRD/CED system based on a passively Q-switched Nd:YAG laser for the measurement of aerosol extinction with a large dynamic range.

INSTRUMENT DESCRIPTION

An overview of the CRD/CED system is shown in Figure 1. The pulsed laser is a frequency-doubled, diode laser-pumped, passively Q-switched Nd:YAG laser (Nanolase NG-1060-100) emitting subnanosecond pulses at 532 nm with a pulse repetition frequency (PRF) of about 14 kHz and a pulse energy of about $0.4 \mu\text{J}$. The all-solid-state technology incorporating passive Q-switching yields a reliable system with a very compact laser head ($\approx 51 \text{ cm}^3$). The laser wavelength was chosen to coincide closely with the spectral maximum of solar irradiance and sensitivity of the human eye for applications in atmospheric radiative transfer and visibility, respectively. It is close to the wavelength 550 nm (typical bandwidth of 50 nm) traditionally used to characterize aerosol optical properties. The laser is mounted together with an optical isolator (Optics For Research IO-3-532-VHP), a lens, and a mechanical chopper (Stanford Research Systems SR540) on a kinematic alignment stage (New Focus 9082). The optical isolator prevents reflections from the CRD/CED cavity from disturbing laser operation, and the lens mode-matches the laser beam into the CRD/CED cavity. The chopper is run at a low frequency ($\approx 15 \text{ Hz}$) to allow for the determination of the background dc signal, which is used to simplify the CRD data analysis and to facilitate phase-sensitive (i.e., lock-in) detection for the CED signal.

The CRD/CED cavity consists of two highly reflecting mirrors (Research Electro Optics; Reflectivity $R \approx 99.995\%$) with a radius of curvature of $r = 1 \text{ m}$ spaced at a distance $L = 0.91 \text{ m}$

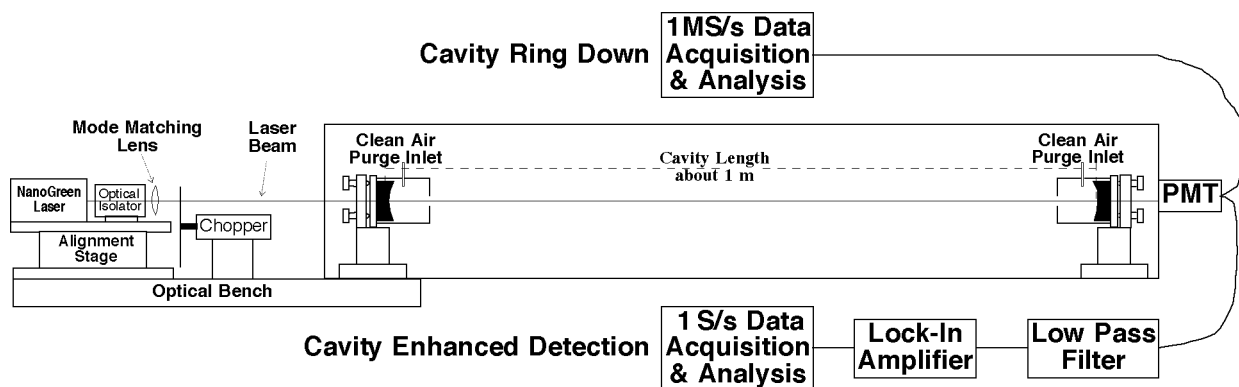


Figure 1. CRD/CED system overview.

from each other, resulting in a near-confocal arrangement. Each mirror is contained in a mirror assembly consisting of a short tube mounted on a mirror mount. The tube has a small opening on the cavity side and is purged with HEPA-filtered air to prevent mirror contamination by aerosol particles. Under conditions of high sample or ambient humidity, the purge air can be dried to prevent potential changes of mirror reflectivity due to water vapor adsorption. The CRD/CED cavity is mounted in a sample cell constructed of a 25 mm diameter stainless steel tube connected on both ends to short 63 mm diameter aluminum extensions that house the mirror assemblies. Windows, sample flow outlets, and feed-throughs are mounted on the two endplates of the cell extensions. One endplate has a photomultiplier tube (PMT) module (Hamamatsu H6780) mounted at its center, and thermocouple, pressure meter (MKS Instruments Type 220 Baratron), and purge flow feed-throughs in its remaining area. In addition, temperature and relative humidity are measured near this plate in the exit flow (Vaisala Humitter 50Y).

The inlet flow is directed through 13 mm diameter tubing into a 13 mm diameter motorized, computer-controlled valve that is used to direct the flow alternately through a HEPA-type particle filter to allow for quantification of the particle contribution to extinction by subtraction. The 13 mm diameter flow line enters the sample cell at its center from above. Here the sample flow is split, with one-half going towards each end of the sample cell. At the each end of the cell, the sample flow exits the cell through 3 exit ports located on a circle around the central optical window at 120° from each other. The sample flow exits the cell outside the optical axis without being obstructed by the central mirror mount. With the sample flow in the opposite direction of the mirror purge flow exiting the mirror assembly, the purge flow quickly and efficiently mixes with the sample flow and does not intrude significantly into the sample volume between the purged volumes. Flow rates for the sample flow are controlled with critical orifices and typically set to 5 l/min on each side for a total of 10 l/min. Flow rates for the mirror purge flow are set and monitored with a needle valve–rotometer combination with typical purge flow rates of 0.05 l/min for each mirror.

A small fraction of the power of each laser pulse enters the CRD/CED cavity through the highly reflecting entrance mirror. While the cavity constitutes a very high finesse interferometer, no interference occurs because the laser pulse is less than one nanosecond (<0.3 m) in length, far less than the cavity roundtrip length of 1.82 m. As the injected laser pulse bounces back and forth between the two mirrors, it loses energy through mirror reflection losses and through extinction by the sample. The energy stored in the cavity is monitored by measuring the transmission of light through the cavity's exit mirror. While the high-speed PMT allows for the discrimination of individual reflections of the pulse contained in the cavity, no additional information is obtained through such a high-speed measurement. Therefore for CRD, the PMT signal is low-pass filtered and then acquired with an A/D converter at 1 MS/s sampling rate, thereby allowing for direct monitoring of the exponential decay of the energy in the

cavity. For CED, the low-pass filtered PMT signal is detected with a lock-in amplifier (Stanford Research Systems SR830) to serve as a measure of cavity extinction.

CRD/CED systems measure total extinction between the mirrors, which is the sum of particle extinction and gaseous extinction. In the green spectral region at 532 nm, significant gaseous extinction is due to scattering by air (13.9 Mm^{-1} at STP; Anderson et al. 1996) and absorption by nitrogen dioxide ($0.402 \text{ Mm}^{-1}/(\text{ppb NO}_2)$ at STP; Harder et al. 1997; Arnott et al. 2000) and ozone ($0.0076 \text{ Mm}^{-1}/(\text{ppb O}_3)$ at STP; Brion et al. 1998). Particle and gaseous contributions can be distinguished by the use of either a particle filter or a gas denuder in the sample stream.

SIGNAL ANALYSIS

CRD Signal Analysis

For highly reflecting mirrors, the time-dependent PMT signal $S(t)$ can be written as

$$S(t) = S_{dc} + S_0 \exp[-\alpha ct] = S_{dc} + S_0 \exp[-(\langle\alpha_S\rangle + \alpha_M)ct], \quad [1a]$$

with

$$\alpha_M = \frac{1 - R}{L} \quad [1b]$$

and

$$\alpha = \langle\alpha_S\rangle + \alpha_M, \quad [1c]$$

where S_{dc} is the *dc* signal offset; S_0 is the signal amplitude; c is the speed of light; R is the mirror reflectivity; L is the distance between the two mirrors; and α is the total decay constant, which is the sum of $\langle\alpha_S\rangle$, the average extinction coefficient of the sample between the resonator mirrors, and α_M , which is due to mirror losses.

The total decay constant α can be calculated from the signal $S(t)$ using Equation (1a). Because the parameters α , S_{dc} , and S_0 are unknown and α cannot be obtained from a linear fit, a nonlinear fitting method such as the Levenberg-Marquardt method (Press et al. 1986) must be used. However, nonlinear fitting methods are slow and may not be well suited for real-time data analysis. Instead, the *dc* signal offset S_{dc} is obtained when the chopper blocks the laser beam. Once S_{dc} is known, it can be subtracted from the signal $S(t)$, and Equation (1) becomes suitable for linear fitting as

$$\ln(S(t) - S_{dc}) = \ln(S_0) - \alpha ct. \quad [2]$$

With $y = \ln(S(t) - S_{dc})$ and $x = -ct$, the total decay constant α and $\ln(S_0)$ are obtained as slope and offset of a linear least square fit, respectively.

The data acquisition system acquires 64000 samples at 1 MS/s and is triggered by the chopper. With the chopper phase set appropriately, the first half of the acquired record contains about 0.032 s of CRD decays (≈ 450 decays at 14 kHz PRF) and the second half contains the dc signal offset S_{dc} . The average of the acquired dc signal offset S_{dc} is subtracted from the CRD record, followed by identification of the parts of the CRD record that contain the exponential decay signal $S(t) - S_{dc}$ for each laser pulse. These parts of the record are used to identify the time of individual laser pulses and to obtain the total decay constant α for each laser pulse with a linear fit to the natural logarithm of the background-corrected signal (Equation (2)). This procedure makes the analysis independent of small amounts of jitter in the timing of the laser pulses. The median value of these ≈ 450 decay constants is used as a robust measure of the total decay constant α for this data record.

CED Signal Analysis

With a laser pulse length much shorter than the cavity roundtrip length $2L$, no interference occurs and the fraction T of the incident pulse energy transmitted through the cavity can be calculated independently of exact laser frequency and cavity length as function of broadband cavity losses. The mirror energy transmissivities are T_{M1} and T_{M2} and the reflectivities R_{M1} , and R_{M2} where the subscript “1” designates the mirror on the laser side and the subscript “2” designates the mirror on the detector side. The cavity roundtrip gain factor g for the pulse energy may be written as

$$\begin{aligned} g &= g_M g_S = (R_{M1} R_{M2}) \exp[-2\alpha_S L] = R_M^2 \exp[-2\alpha_S L] \\ &= \exp[\ln(R_M^2) - 2\alpha_S L], \end{aligned} \quad [3a]$$

where R_M is the geometric mean of R_{M1} and R_{M2} , and

$$g_M = (R_{M1} R_{M2}) = R_M^2 = \exp[\ln(R_{M1} R_{M2})] = \exp[\ln(R_M^2)] \quad [3b]$$

and

$$g_S = \exp[-2\alpha_S L] \quad [3c]$$

are the roundtrip gain factors due to mirror reflectivity (g_M) and due to extinction of the sample between the mirrors (g_S), respectively. For passive cavities considered here the roundtrip gain factor g as well as its components g_M and g_S are smaller than unity, indicating net loss, and a corresponding loss factor $g_L = 1 - g$ can be defined.

When one laser pulse with energy E is incident upon the cavity, a fast detector can resolve a series of pulses on the detector side of the cavity. The first pulse has an energy E_0 and results from direct transmission of the laser pulse through the two mirrors, the second pulse has in addition undergone one roundtrip (i.e., two reflections, one on each mirror) in the cavity, and the i th pulse has in addition undergone $(i - 1)$ roundtrips in the cavity.

The energy E_0 of the first pulse may be written as the product of the energy of the incident laser pulse E , the product $T_{M1} T_{M2}$ of the two mirror transmissivities and the one-way extinction $\exp[-\alpha_S L]$ as

$$E_0 = E T_{M1} T_{M2} \exp[-\alpha_S L] = E T_M^2 \exp[-\alpha_S L] = E T_M^2 \sqrt{g_S}, \quad [4a]$$

where T_M is the geometric mean of T_{M1} and T_{M2} . The energy of the i th pulse can be written as that of the first pulse multiplied by the roundtrip gain g to the i th power, that is,

$$E_i = E_0 g^i. \quad [4b]$$

The total energy E_t transmitted through the cavity from one incident laser pulse is obtained as a convergent series of the energies of the individual transmitted pulses

$$E_t = \sum_{i=0}^{\infty} E_i = E_0 \sum_{i=0}^{\infty} g^i. \quad [4c]$$

With the use of the power series,

$$\sum_{i=0}^{\infty} x^i = \frac{1}{1-x} \quad \forall x < 1, \quad [5a]$$

and the cavity energy transmissivity T , defined as

$$T = \frac{E_t}{E}, \quad [5b]$$

it follows that

$$T = \frac{T_M^2 \sqrt{g_S}}{1-g} = \frac{T_M^2 \sqrt{g_S}}{1-g_M g_S}. \quad [5c]$$

As the mirror transmissivity T_M is not known, there is no need for an absolute measurement of the cavity energy transmissivity T . Instead, a signal S proportional to T is measured, with S being defined as

$$S = k \frac{T}{T_M^2} = k \frac{E_t}{E T_M^2}, \quad [6a]$$

where k is an unknown proportionality constant. This yields

$$\frac{S}{k} = \frac{\sqrt{g_S}}{1-g_M g_S}. \quad [6b]$$

To solve for the roundtrip gain factor g_S due to the sample between the mirrors, this is rewritten as quadratic equation for g_S :

$$g_S^2 - g_S \left(\frac{2}{g_M} - \frac{k^2}{S^2 g_M^2} \right) + \frac{1}{g_M^2} = 0, \quad [7a]$$

which yields one physical solution with $g_S \leq 1$ as

$$g_S = \frac{2g_M + \left(\frac{k}{S}\right)^2 - \frac{k}{S}\sqrt{4g_M + \left(\frac{k}{S}\right)^2}}{2g_M^2}. \quad [7b]$$

With $g_S = \exp[-2\alpha_S L]$ it follows

$$\alpha_S = \frac{1}{2L} \ln \left(\frac{2g_M^2}{2g_M + \left(\frac{k}{S}\right)^2 - \frac{k}{S}\sqrt{4g_M + \left(\frac{k}{S}\right)^2}} \right), \quad [8]$$

and the sample decay constant α_S can be obtained after determining the unknown values of k and g_M through calibration using, for example, two gases with different extinction coefficients. The relationship between CED signal S and sample decay constant α_S is shown in Figure 2 as solid line and is further discussed in the following section.

CED Approximations

The CED signal is described by Equation (6b), and the solutions for the gain g_S and the extinction α_S between the cavity mirrors are given by Equations (7b) and (8), respectively. In addition to these exact expressions, simple approximations for small and large extinction are considered in the following to facilitate better understanding.

In the case of small extinction ($g_S \approx 1$ and consequently $k/S \ll 1$), k/S can be approximated as

$$\frac{k}{S} \approx 1 - g_M g_S, \quad [9a]$$

yielding

$$g_S \approx \frac{1}{g_M} \left(1 - \frac{k}{S} \right) \quad \text{and} \quad \alpha_S \approx \frac{1}{2L} \ln \left(\frac{g_M}{1 - \frac{k}{S}} \right), \quad [9b]$$

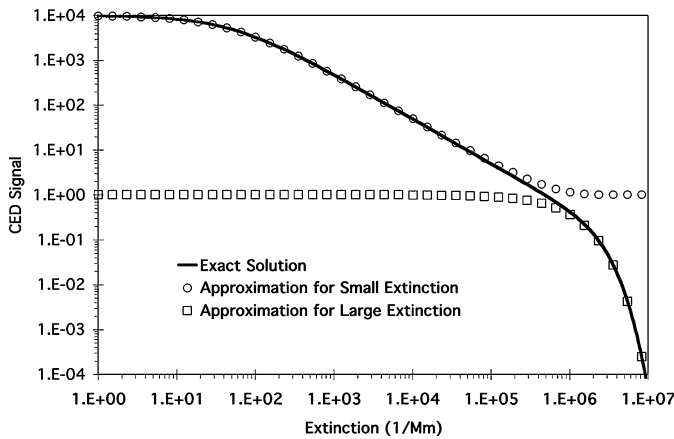


Figure 2. CED signal as function of extinction for cavity length of $L = 1$ m, mirror reflectivity $R_M = 0.99995$ (i.e., $\alpha_M = 50 \text{ Mm}^{-1}$), and a proportionality constant $k = 1$.

or the reverse relationships as

$$S \approx \frac{k}{1 - g_M g_S} = \frac{k}{1 - g_M \exp[-2\alpha_S L]}. \quad [9c]$$

This relationship is shown in Figure 2 as open circles demonstrating good agreement with the exact formula below about 10^5 Mm^{-1} ($< 0.1 \text{ m}^{-1}$) for a cavity length of 1 m. In this region, the CED signal depends strongly on sample extinction when mirror losses can be neglected (i.e., $\alpha_S \gg \alpha_M$), while this dependence decreases when mirror losses start dominating the total losses. In the case of large extinction ($g_S \approx 0$ and consequently $kS \gg 1$), S/k can be approximated as

$$\frac{S}{k} = \frac{\sqrt{g_S}}{1 - g_M g_S} \approx \sqrt{g_S}, \quad [10a]$$

yielding

$$g_S \approx \left(\frac{S}{k} \right)^2 \quad \text{and} \quad \alpha_S \approx \frac{1}{L} \ln \left(\frac{k}{S} \right), \quad [10b]$$

or the reverse relationships as

$$S \approx k\sqrt{g_S} = k \exp[-\alpha_S L]. \quad [10c]$$

For large extinction, g_S is proportional to the square of the total transmitted energy per pulse E_t and independent of mirror reflectivity (with the exception that T^2 depends on the reflectivity). This limit corresponds to single-pass extinction, i.e., the extinction is so large that most of the energy, E_t , is contributed by the single-pass energy, E_0 , and the contribution from pulses that have undergone one or more cavity roundtrips can be neglected due to the large extinction in the cavity. In other words, in the limit of large extinction no cavity enhancement takes place and the system performs a single-pass extinction measurement as described by Beer's law in Equation (10c). This relationship is shown in Figure 2 as open squares and demonstrates good agreement with the exact formula above about 10^6 Mm^{-1} ($< 1 \text{ m}^{-1}$) for a cavity length of 1 m.

INSTRUMENT CALIBRATION

The measurement of extinction with CRD/CED is different from the measurement of the scattering component of extinction with an integrating nephelometer, not only due to the inclusion of absorption but also due to the different calibration procedures, which are inherently simpler for CRD. Nephelometers measure the transfer function between a light source and a detector for the scattered light due to light scattering in the medium of interest. This transfer function can be deduced from the measured scattering signal if both the many efficiencies and sensitivities of the light source, optical elements, and detector and dc offsets due to, for example, wall scattering are known. As these factors are difficult to determine, they are generally not known, and the nephelometer is calibrated with two media to determine a linear

function between raw signal and scattering coefficient defined by its slope and offset (Anderson et al. 1996; Heintzenberg and Charlson 1996). CED calibration is similar to nephelometer calibration because two calibration constants (i.e., k and g_M) need to be determined. For CRD, extinction is not a function of signal amplitude but of signal decay in the time domain, so only the extinction offset due to inherent cavity (i.e., mirror) losses needs to be determined. This can be done conveniently with a single calibration gas such as filtered (zero) air of known density (i.e., pressure and temperature). In addition, a mechanically stable CRD system contained in a good vacuum system can be used to measure absolute extinction coefficients for gases without a priori knowledge of the extinction of a calibration medium (Naus and Ubachs 2000). Therefore, CRD systems have the potential for a more direct and potentially more accurate measurement of scattering coefficients of gases commonly used for the calibration of nephelometers (Anderson et al. 1996).

For this discussion of CRD/CED calibration, it is initially assumed that the measurement volume between the mirrors is filled with a single homogeneous medium (Single Medium; Mirrors Not Purged). This discussion is then extended to a special case of an inhomogeneous medium, namely different regions of the measurement volume being filled by the sample and a purge gas (Dual Media; Mirrors Purged).

Single Medium; Mirrors Not Purged

If the measurement volume is filled with a single, homogeneous medium, the total decay constant α can be written as

$$\alpha = \alpha_S + \alpha_M = (\alpha_g + \alpha_p) + \alpha_M, \quad [11]$$

where $\alpha_M = (1 - R)/L$ is due to mirror losses and α_S is the extinction of sample filling the cell. This extinction α_S has two components, the extinction α_g due to the gaseous components and the extinction α_p due to the suspended particles.

For the CRD calibration only one calibration medium and no knowledge of the distance L between the mirrors is needed, while for the CED calibration two calibration media and knowledge of L is needed.

CRD Calibration, Single Medium. To obtain α_S from α , α_M must be determined by filling the cell with a calibration medium with known extinction α_{S_cal} such as vacuum ($\alpha_{S_cal_v} = 0$) or zero air ($\alpha_{S_cal_air} = 13.85 \text{ Mm}^{-1} \pm 0.24\%$ at STP and 532 nm; this assumes NO_2 and O_3 free air; Anderson et al. 1996). Measuring the total decay constant α_{cal} while the cell is filled with a calibration medium with known extinction coefficients α_{S_cal} yields the mirror contribution α_M as

$$\alpha_M = \alpha_{cal} - \alpha_{S_cal}. \quad [12a]$$

Alternatively, two or more calibration gases could be used and the mirror contribution α_M could be obtained as the y -offset of a linear regression using the measured total decay constants α_{cal_i} as y values and the known extinction coefficients $\alpha_{S_cal_i}$ of the

calibration media as x values. In this case, the linear regression slope should equal one, and deviations from this value can be used to evaluate measurement errors and errors in the “known” extinction coefficients of the calibration media.

Once calibrated, the extinction α_S due to the medium between the mirrors is obtained as

$$\alpha_S = \alpha - \alpha_M = \alpha - (\alpha_{cal} - \alpha_{S_cal}), \quad [12b]$$

assuming that α_M has not changed since the calibration.

The extinction α_p due to the suspended particles can be obtained as the difference between the extinction of the sample and the extinction of the sample’s gaseous component (i.e., the sample with particles removed through filtering) as

$$\begin{aligned} \alpha_p &= (\alpha_g + \alpha_p) - \alpha_g = \alpha_S - \alpha_{S_filtered} = (\alpha - \alpha_M) \\ &\quad - (\alpha_{filtered} - \alpha_M) = \alpha - \alpha_{filtered}. \end{aligned} \quad [13]$$

For this measurement of the particulate component of the extinction, the calibration terms or mirror contributions α_M cancel and no calibration with a medium with known extinction is needed. Instead, the measurement of the extinction $\alpha_{filtered}$ of the filtered medium serves as calibration for the determination of the particulate extinction. This calibration is valid as long as the sum of the gaseous sample extinction α_g and the mirror contribution α_M stays constant.

CED Calibration. To measure the roundtrip gain factor, g_S (g_S is smaller than unity, corresponding to a loss), due to the extinction between the mirrors and thereby the extinction coefficient, α_S , requires knowledge of the roundtrip gain factors due to mirror reflectivity, $g_M = (R_{M1} R_{M2})$, and the proportionality constant, k , in the energy detection that includes variables such as laser pulse energy, detector sensitivity, mode matching, alignment, and mirror transmission. First, the roundtrip gain factors, $g_{S_cal_i}$, of the calibration media, i , are calculated through Equation (3c) from their known extinction coefficients, $\alpha_{S_cal_i}$, and the distance, L , between the two cavity mirrors. Then, the unknown parameters, g_M and k , can be determined by measuring the CED signals, S_i , for two calibration media. The proportionality constant, k , is obtained from Equation (6b) as

$$k = \frac{\frac{1}{g_{S_cal_1}} - \frac{1}{g_{S_cal_2}}}{\frac{1}{S_1 \sqrt{g_{S_cal_1}}} - \frac{1}{S_2 \sqrt{g_{S_cal_2}}}}, \quad [14a]$$

and the roundtrip gain factor due to mirror losses, $g_M = R_1 R_2$, can be calculated from Equation (6b) as

$$g_M = \frac{\frac{S_1}{\sqrt{g_{S_cal_1}}} - \frac{S_2}{\sqrt{g_{S_cal_2}}}}{S_1 \sqrt{g_{S_cal_1}} - S_2 \sqrt{g_{S_cal_2}}}. \quad [14b]$$

If more than two calibration media are used, Equation (6b) may be rewritten as

$$\frac{1}{g_S} = g_M + k \frac{1}{S\sqrt{g_S}}, \quad [15]$$

and with $1/g_S$ as y values and $1/(Sg_S^{0.5})$ as x values, g_M and k may be obtained as y offset and slope of a linear regression.

Once g_M and k have been obtained through calibration, the sample extinction, α_S , is calculated from Equation (8) and extinction, α_p , due to the suspended particles can be obtained with Equation (13).

Similar to nephelometer calibration, filtered air and carbon dioxide (CO₂) can be used as calibration media in the posthalo-carbon era. Extinction coefficients for these media are well known (Anderson et al. 1996), and values for 532 nm can be calculated from those at 550 nm through the λ^{-4} approximation of the wavelength dependence of molecular scattering. At STP and 532 nm, this yields $\alpha_{S_cal_air_STP} = 13.85 \text{ Mm}^{-1} \pm 0.24\%$ and $\alpha_{S_cal_CO2_STP} = 35.87 \text{ Mm}^{-1} \pm 0.90\%$. However, in the case of a dual CRD/CED instrument, it may be simpler to calibrate the CRD measurements with one calibration medium and to use the calibrated CRD measurements of at least two samples (with a priori unknown extinction) to calibrate the CED measurements.

Dual Media, Mirrors Purged. For our cell design, calibration is more complex due to the purged regions adjacent to the mirrors. These purged regions prevent mirror contamination and keep the mirror losses (i.e., α_M) constant. In our design, there are two different media between the mirrors, the purged regions with extinction coefficient, α_{S_purge} , in the short purged tubes (each of length L_{purge}) of the mirror assembly and the sample region of length, L_S , with extinction coefficient, α_{S_S} , between the purged tubes, where

$$L = L_S + 2L_{purge}. \quad [16a]$$

The spatially averaged extinction coefficient, $\langle \alpha_S \rangle$, can be written as

$$\begin{aligned} \langle \alpha_S \rangle &= \frac{\alpha_{S_S} L_S + 2\alpha_{S_purge} L_{purge}}{L_S + 2L_{purge}} \\ &= \frac{\alpha_{S_S} L_S + 2\alpha_{S_purge} L_{purge}}{L}. \end{aligned} \quad [16b]$$

Calibration can be performed with uniform media (at least one for CRD, at least two for CED), filling the whole length, L , including the purged regions. In this case, the calibration constants for CRD and CED are obtained just as in the “single medium” case.

Once calibrated, Equation (16b) can be used to calculate the sample extinction coefficient, α_{S_S} , as

$$\alpha_{S_S} = \langle \alpha_S \rangle + \left[\frac{2L_{purge}}{L_S} (\langle \alpha_S \rangle - \alpha_{purge}) \right], \quad [16c]$$

where the term in the square bracket is the purge correction. The extinction coefficient, α_{purge} , in the purged regions must be known for this calculation. This is commonly achieved by using zero air of known density to purge the mirrors.

Alternatively, the mirror purge can be maintained during both calibration and measurement. In this case, the purged region and its associated extinction can just be treated jointly with the mirror losses resulting in a joint mirror-purge extinction, α_{M_purge} , where

$$\alpha_{M_purge} = \frac{(1 - R) + 2\alpha_{S_purge} L_{purge}}{L}. \quad [17]$$

The extinction, α_p , due to the suspended particles can be obtained from Equations (13) and (16c) as the difference between the extinction of the sample and the extinction of the sample's gaseous component (i.e., the sample with particles removed through filtering) as

$$\begin{aligned} \alpha_p &= (\langle \alpha_g \rangle + \langle \alpha_p \rangle) - \langle \alpha_g \rangle = \alpha_{S_S} - \alpha_{S_filtered} \\ &= \frac{L}{L_S} (\langle \alpha_S \rangle - \langle \alpha_{S_filtered} \rangle) = \frac{L}{L_S} (\alpha - \alpha_{filtered}). \end{aligned} \quad [18]$$

For this measurement of the particulate component of the extinction, the calibration terms or mirror contributions, α_M , cancel, and no calibration with a medium with known extinction is needed. Instead, the measurement of the extinction, $\alpha_{filtered}$, of the filtered medium serves as calibration for the determination of the particulate extinction. This calibration is similar to the calibration without mirror purge (Equation (13)) but adds a factor (i.e., L/L_S) to account for the particle-free (purged) region adjacent to the mirrors.

EXAMPLE DATA AND DISCUSSION

The combined CRD/CED system has been used in multiple measurement applications, and example data from a couple of them are discussed here.

Calibration with Two Calibration Gases

During the Reno Aerosol Optics Study (RAOS; Sheridan et al. 2005), a calibration of the CRD/CED instrument was performed, using filtered air for the CRD calibration and filtered air and carbon dioxide (CO₂) for the CED calibration. In either case, the whole extinction cell is filled with the calibration medium and CRD/CED measurements are made.

For CRD, filtered air with an extinction coefficient of $\alpha_{S_cal_air} = 10.78 \text{ Mm}^{-1}$ at its density in the CRD/CED cell ($T = 297.1 \text{ K}$ and $p = 857.5 \text{ mB}$) is used for calibration. The CRD measurement yields a total decay constant $\alpha_{cal_air} = 66.03 \text{ Mm}^{-1}$. Equation (12a) is used to calculate the mirror contribution of $\alpha_{M_air} = 55.25 \text{ Mm}^{-1}$ and the CRD measurement is calibrated. For the CED calibration, the cell was also filled with CO₂ ($\alpha_{S_cal_CO2} = 28.42 \text{ Mm}^{-1}$ at its density in the CRD/CED cell ($T = 297.2 \text{ K}$ and $p = 873.4 \text{ mB}$)) and a CRD measurement of CO₂ extinction ($\alpha_{cal_CO2} = 83.30 \text{ Mm}^{-1}$) yields $\alpha_{M_CO2} = 54.88 \text{ Mm}^{-1}$, well within 1% of the filtered air CRD

calibration. In addition, the measurement of the CO_2 extinction coefficient with filtered air calibration and of the filtered air extinction coefficient with CO_2 calibration are well within the uncertainties (i.e., $\pm 0.24\%$ for air, $\pm 0.9\%$ for CO_2 ; Anderson et al. 1996) of the literature values for CO_2 and filtered air extinction.

For the CED calibration, Equation (3c) is used to calculate the roundtrip gain factors, and $g_{S_{cal,air}}$ and $g_{S_{cal,CO_2}}$ are calculated for filtered air and CO_2 from the distance $L = 0.91$ m between the mirrors and the extinction coefficients of filtered air and CO_2 at temperature and pressure conditions during calibration. This yields roundtrip gain factors of $g_{S_{cal,air}} = 0.9999803$ and $g_{S_{cal,CO_2}} = 0.9999482$ for $\alpha_{S_{cal,air}} = 10.78 \text{ Mm}^{-1}$ (for $T = 297.1 \text{ K}$ and $p = 857.5 \text{ mB}$), and $\alpha_{S_{cal,CO_2}} = 28.42 \text{ Mm}^{-1}$ (for $T = 297.2 \text{ K}$ and $p = 873.4 \text{ mB}$). Using the CED signals measured during calibration (i.e., $S_{air} = 0.1984 \text{ V}$ and $S_{CO_2} = 0.1576 \text{ V}$), the two CED calibration constants k and g_M can be calculated from Equations (14a) and (14b), as $k = 0.0246 \text{ mV}$ and $g_M = 0.9998956$. The round trip gain factor due to mirror reflectivity obtained from the CED calibration $g_M = 0.9998956$ is in good agreement with one calculated from the CRD calibration by converting the mirror contribution to extinction α_M to a roundtrip gain factor $g_{M,CRD} = (1 - L\alpha_M)^2 = 0.9998998$. Both CED and CRD calibrations yield the geometric mean of the two mirror reflectivities as $R_M = 99.995\%$.

Instrument Noise and Stability

During routine operation the CRD/CED instrument is zeroed with filtered air every hour to minimize potential stability problems. However, during RAOS the instrument was operated for about two days, continually measuring filtered air extinction. To evaluate instrument noise and stability, CRD/CED data averaged over 1 min intervals and corrected to STP conditions are shown in Figure 3 for a 6 h period starting 36 h after the last instrument calibration together with the filtered air calibration

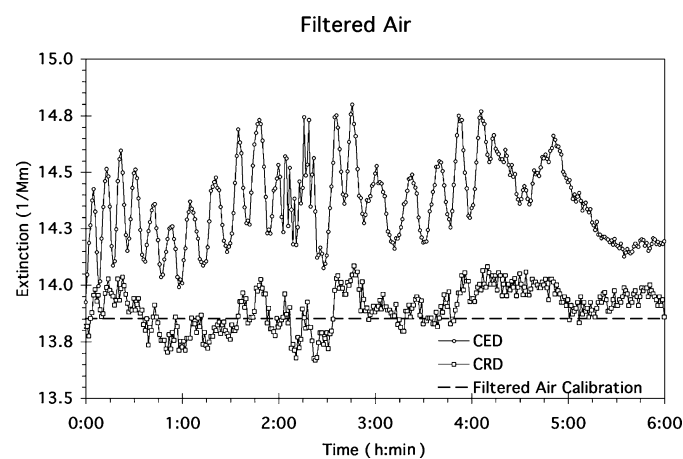


Figure 3. Extinction of filtered air measured with CRD and CED to evaluate instrument noise and stability. This data record, showing 1 min averages, starts 36 h after the last instrument calibration.

value of 13.85 Mm^{-1} at STP. The average results over this 6 h period are 13.90 Mm^{-1} for CRD and 14.36 Mm^{-1} for CED. This dataset demonstrates excellent stability (0.05 Mm^{-1}) for CRD and good stability (0.5 Mm^{-1}) for CED even questioning the need for hourly calibrations with filtered air. Instrument noise is quantified by the standard deviation from the mean for the 1 min data points. The standard deviation is 0.09 Mm^{-1} for CRD and 0.18 Mm^{-1} for CED. In summary, both measurement methods easily fulfill the need for a measurement sensitivity of 1 Mm^{-1} , as described in the introduction, even without frequent calibration. The CRD measurement is both more stable and has less noise as the CED measurement, which depends on stability of the laser power and the detector responsivity.

Extinction Measurements

The calibrated CRD/CED system was used during RAOS for the time-resolved extinction measurement of laboratory-generated aerosols. As examples, CRD and CED measurements of the average cell extinction, $\langle \alpha_S \rangle$, are compared with each other over 4 h with 1 min time resolution. Figures 4 and 5 show CRD/CED data for diesel exhaust and ammonium sulfate ($(\text{NH}_4)_2\text{SO}_4$) aerosols, respectively. Both cases show excellent correlation ($R^2 > 0.999$) between CRD and CED data and excellent quantitative agreement with a regression slope within 2% of one and an offset of less than 1% of the maximum value. However, the CED extinction is somewhat noisier than the CRD extinction at low values due to its uncorrected dependence on the laser power.

The CRD/CED system was also used during the Combustion Aerosol Optics Study (CAOS) conducted jointly with Colorado State University and the U.S. Forest Service (USFS) at the USFS Fire Science Laboratory in Missoula, MT. During this study, very large extinction values were encountered, demonstrating the large dynamic range of the CED approach. In addition, a

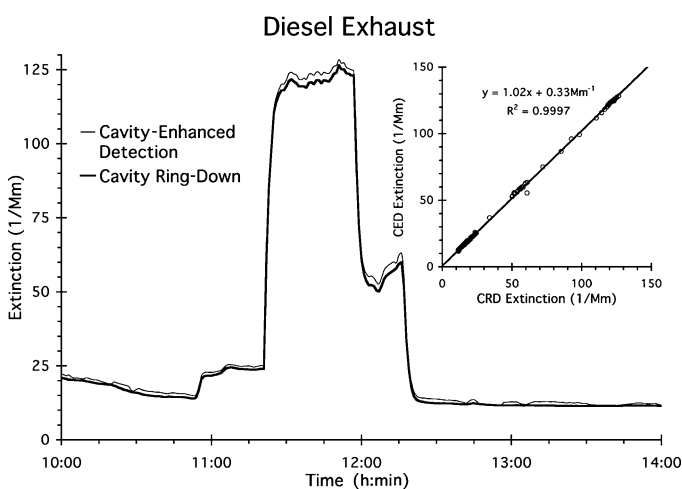


Figure 4. Extinction of diesel exhaust measured with CRD and CED after CRD calibration with filtered air and CED calibration with filtered air and carbon dioxide.

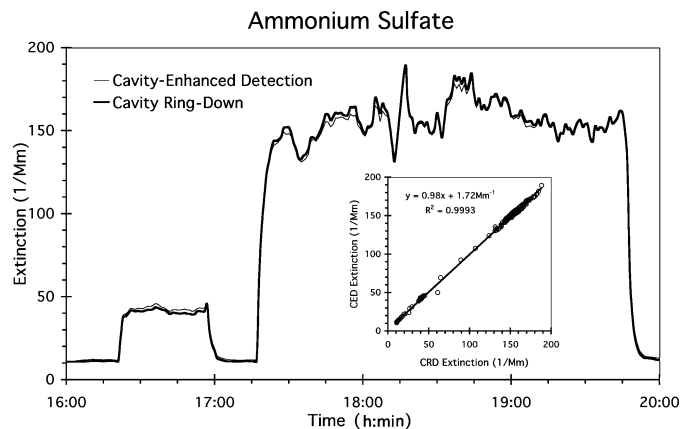


Figure 5. Extinction of ammonium sulfate measured with CRD and CED after CRD calibration with filtered air and CED calibration with filtered air and carbon dioxide.

simpler calibration approach utilizing filtered air for the CRD calibration and filtered air and CRD measurements for the CED calibration was demonstrated.

Figure 6 plots the average cell extinction, $\langle \alpha_S \rangle$, from CRD/CED measurements of smoke from the combustion of White Pine needles with 10 s time resolution. During the initial minutes (15:50:00–15:53:50), the extinction of filtered ambient air with an extinction coefficient of $\alpha_{S,cal,air} = 11.16 \text{ Mm}^{-1}$ at its density in the CRD/CED cell ($T = 300.3 \text{ K}$ and $p = 897.3 \text{ mB}$) is measured for CRD calibration. For the CED calibration, the cell was also filled with ambient air, and the CRD measurement of ambient air from 15:54:20–15:56:40 yields an extinction of 21.63 Mm^{-1} . This value is used as second value for CED calibration from the CED signals of 10.93 mV (filtered air), and 9.99 mV (ambient air), yielding CED calibration constants of $k = 0.00223 \text{ mV}$ and $g_M = 0.9998162$. The fire is ignited at

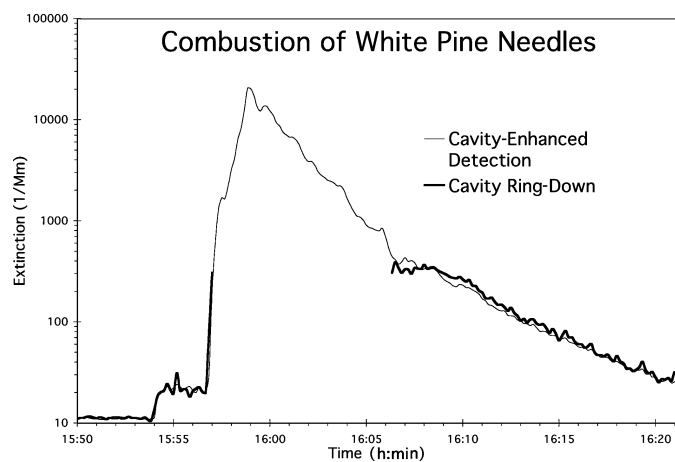


Figure 6. Extinction of smoke from the combustion of White Pine needles measured with CRD and CED after CRD calibration with filtered air and CED calibration with filtered air and ambient air extinction as measured by CRD.

about 15:56:40, and the measured extinction begins to rise dramatically shortly thereafter (Figure 6). Note that due to the rapid decrease in extinction, the agreement between CRD and CED between 16:05 and 16:10 is not as good as elsewhere. This is largely due to the somewhat different time response of the two measurement methods. The CRD instrument was originally set up for measurements in the ambient atmosphere and does not function properly for extinction values above about 500 Mm^{-1} . While increasing the sampling rate and decreasing the analog time constant of the data acquisition could increase this upper limit, the CED measurement offers a simple alternative for situations requiring a larger dynamic range. Figure 6 demonstrates good agreement between CRD and CED measurements below 500 Mm^{-1} and the suitability of the CED instrument for the measurement of very large extinction ($> 20,000 \text{ Mm}^{-1}$) as encountered in biomass combustion plumes.

SUMMARY AND CONCLUSIONS

An instrument for the in situ measurement of extinction, ranging from very low extinction in the near Rayleigh-limited ambient atmosphere to very high extinction in combustion plumes, has been described and demonstrated. This instrument utilizes cavity ring-down (CRD) for the measurement of relatively low ambient extinction by determining the photon lifetime in a high quality optical resonator. The use of an optical chopper facilitates determination of the baseline of the ring-down signal and thereby the use of linear fitting procedures for the determination of photon lifetime. By employing laser pulses shorter than the resonator length, the measurement is made without encountering complications due to optical interference. The interference-free nature of this measurement also makes it possible to add a cavity-enhanced detection (CED) measurement of extinction by the simple addition of low-frequency phase-sensitive detection. The availability of CED in addition to CRD has made it possible to limit the potential for systematic errors by demonstrating excellent agreement between CRD and CED measurements and also for a much-increased dynamic measurement range.

REFERENCES

- Anderson, T. L., Covert, D. S., Marshall, S. F., Laucks, M. L., Charlson, R. J., Waggoner, A. P., Ogren, J. A., Caldwell, R., Holm, R. L., Quant, F. R., Sem, G. J., Wiedensohler, A., Ahlquist, N. A., and Bates, T. S. (1996). Performance Characteristics of a High-Sensitivity, Three-Wavelength, Total Scatter/Backscatter Nephelometer, *J. Atmos. Ocean. Technol.* 13:967–986.
- Arnott, W. P., Moosmüller, H., and Walker, J. W. (2000). Nitrogen Dioxide and Kerosene-Flame Soot Calibration of Photoacoustic Instruments for Measurement of Light Absorption by Aerosols, *Rev. Sci. Instrum.* 71:4545–4552.
- Bates, D. R. (1984). Rayleigh Scattering by Air, *Planet. Space Sci.* 32:785–790.
- Brion, J., Chakir, A., Charbonnier, J., Daumont, D., Parisse, C., and Malicet, J. (1998). Absorption Spectra for the Ozone Molecule in the 350–830 nm Region, *J. Atmos. Chem.* 30:291–299.
- Bucholtz, A. (1995). Rayleigh-Scattering Calculations for the Terrestrial Atmosphere, *Appl. Opt.* 34:2765–2773.
- Chetwynd, J. G., Wang, J., and Anderson, G. P. (1994). FASCODE: An Update and Applications in Atmospheric Remote Sensing, *Proc. SPIE* 2266:613–619.

- Chow, J. C., Bachman, J. D., Wierman, S. S. G., Mathai, C. V., Malm, W. C., White, W. H., Mueller, P. K., Kumar, N., and Watson, J. G. (2002). 2002 Critical Review Discussion—Visibility: Science and Regulation, *J. Air & Waste Manage. Assoc.* 52:973–999.
- Davidson, J. A., Cantrell, C. A., McDaniel, A. H., Shetter, R. E., Madronich, S., and Calvert, J. G. (1988). Visible-Ultraviolet Absorption Cross Sections for NO₂ as a Function of Temperature, *J. Geophys. Res.* 93:7105–7112.
- Demtröder, W. (2002). *Laser Spectroscopy: Basic Concepts and Instrumentation*. Springer Verlag Berlin, Heidelberg, New York.
- Harder, J. W., Brault, J. W., Johnston, P. V., and Mount, G. H. (1997). Temperature Dependent NO₂ Cross Sections at High Spectral Resolution, *J. Geophys. Res.* 102:3861–3879.
- Heintzenberg, J., and Charlson, R. J. (1996). Design and Application of the Integrating Nephelometer: A Review, *J. Atmos. Ocean. Technol.* 13:987–1000.
- Herriott, D. R., and Schulte, H. J. (1965). Folded Optical Delay Lines, *Appl. Opt.* 4:883–889.
- Jain, A. K., Briegleb, B. P., Minschwaner, K., and Wuebbles, D. J. (2000). Radiative Forcings and Global Warming Potentials of 39 Greenhouse Gases, *J. Geophys. Res.* 105:20773–20790.
- Knollenberg, R. G. (1982). A Laser Cavity Extinction Photometer for Measurements of Extinction Coefficient and Visual Range. In *Light Absorption by Aerosol Particles*, edited by H. E. Gerber and E. E. Hindman. Spectrum Press, Hampton, VA, pp. 65–69.
- Lubin, D., Vogelmann, A., Lehr, P. J., Kressin, A., Ehranjian, J., and Ramanathan, V. (2000). Validation of Visible/Near-IR Atmospheric Absorption and Solar Emission Spectroscopic Models at 1 cm⁻¹ Resolution, *J. Geophys. Res.* 105:22445–22454.
- McManus, J. B., Kebabian, P. L., and Zahniser, M. S. (1995). Astigmatic Mirror Multipass Absorption Cells for Long-Path-Length Spectroscopy, *Appl. Opt.* 34:3336–3348.
- Molenaar, J. V., Dietrich, D. L., Tree, R. M., Malm, W. C., and Persha, G. (1989). “Application of a Long Range Transmissometer to Measure the Ambient Atmospheric Extinction Coefficient in Remote Pristine Environments.” In *Visibility and Fine Particles*, edited by C. V. Mathai. Air & Waste Management Association, Pittsburgh, PA, TR-17, pp. 305–317.
- Naus, H., and Ubachs, W. (2000). Experimental Verification of Rayleigh Scattering Cross Sections, *Opt. Lett.* 25:347–349.
- O’Keefe, A., and Deacon, D. A. G. (1988). Cavity Ring-Down Optical Spectrometer for Absorption Measurements Using Pulsed Laser Sources, *Rev. Sci. Instrum.* 59:2544–2551.
- Paul, J. B., Lapson, L., and Anderson, J. G. (2001). Ultrasensitive Absorption Spectroscopy with a High-Finesse Optical Cavity and Off-Axis Alignment, *Appl. Opt.* 40:4904–4910.
- Press, W. H., Flannery, B. P., Teukolsky, S. A., and Vetterling, W. T. (1986). *Numerical Recipes: The Art of Scientific Computing*. Cambridge University Press, New York, pp. xx, 818.
- Ramponi, A. J., Milanovitch, F. P., Kan, T., and Deacon, D. (1988). High Sensitivity Atmospheric Transmission Measurements Using a Cavity Ringdown Technique, *Appl. Opt.* 27:4606–4608.
- Reddy, M. S., and Venkataraman, C. (2000). Atmospheric Optical and Radiative Effects of Anthropogenic Aerosol Constituents from India, *Atmos. Environ.* 34:4511–4523.
- Romanini, D., Kachanov, A. A., and Stoeckel, F. (1997). Cavity Ringdown Spectroscopy: Broad Band Absolute Absorption Measurements, *Chem. Phys. Lett.* 270:546–550.
- Rothman, L. S., Rinsland, C. P., Goldman, A., Massie, S. T., Edwards, D. P., Flaud, J.-M., Perrin, A., Camy-Peyret, C., Dana, V., Mandin, J.-Y., Schroeder, J., McCann, A., Gamache, R. R., Wattson, R. B., Yoshino, K., Chance, K. V., Jucks, K. W., Brown, L. R., Nemtchinov, V., and Varanasi, P. (1998). The HITRAN Molecular Spectroscopic Database and HAWKS (HITRAN Atmospheric WorkStation): 1996 Edition, *J. Quantitative Spectroscopy Radiative Trans.* 60:665–710.
- Sappety, A. D., Hill, E. S., Settersten, T., and Linne, M. A. (1998). Fixed-Frequency Cavity Ringdown Diagnostic for Atmospheric Particulate Matter, *Opt. Lett.* 23:954–956.
- Schott, J. R. (1997). *Remote Sensing : The Image Chain Approach*. Oxford University Press, New York, pp. xiv, 394.
- Sheridan, P. J., Arnott, W. P., Ogren, J. A., Andrews, E., Atkinson, D. B., Covert, D. S., Moosmüller, H., Petzold, A., Schmidt, B., Strawa, A. W., Varma, R., and Virkkula, A. (2005). The Reno Aerosol Optics Study: Overview and Summary of Results, *Aerosol Sci. Technol.* 39:1–16.
- Smith, J. D., and Atkinson, D. B. (2001). A Portable Pulsed Cavity Ring-Down Transmissometer for Measurement of the Optical Extinction of the Atmospheric Aerosol, *Analyst* 126:1216–1220.
- Strawa, A. W., Castaneda, R., Owano, T., Baer, D. S., and Paldus, B. A. (2002). The Measurement of Aerosol Optical Properties Using Continuous Wave Cavity Ring-Down Techniques, *J. Atmos. Ocean. Technol.*, 20:454–465.
- Thompson, J. E., Smith, B. W., and Winefordner, J. D. (2002). Monitoring Atmospheric Particulate Matter through Cavity Ring-Down Spectroscopy, *Anal. Chem.* 74:1962–1967.
- Watson, J. G. (2002). 2002 Critical Review—Visibility: Science and Regulation, *J. Air Waste Manage. Assoc.* 52:626–713.
- White, J. U. (1976). Very Long Optical Paths in Air, *J. Opt. Soc. Am.* 66:411–416.
- Ye, J., L.-S. Ma, and Hall, J. L. (1996). Sub-Doppler Optical Frequency Reference at 1.064 μm by Means of Ultrasensitive Cavity-Enhanced Frequency Modulation Spectroscopy of a C₂HD Overtone Transition, *Opt. Lett.* 21:1000–1002.